Preparation of gold tetrananocages and their photothermal effect*

Yin Nai-Qiang(尹乃强)[a], Liu Ling(刘 玲)[a], Lei Jie-Mei(雷洁梅)[a],
Jiang Tong-Tong(蒋童童)[a], Zhu Li-Xin(朱立新)[b]†, and Xu Xiao-Liang(许小亮)[a]‡

[a] *Department of Physics, University of Science and Technology of China, Hefei* 230026, *China*
[b] *Center Laboratory, First Affiliated Hospital of Anhui Medical University, Hefei* 230022, *China*

(Received 13 January 2013; revised manuscript received 18 April 2013)

A gold tetrahedral nanocage, i.e., a tetrananocage, that converts near-infrared (NIR) light into heat was fabricated by using a simple method. Silver tetrahedra with good homogeneity and dispersity were synthesized by a hydrothermal route. Gold tetrananocages were obtained using a galvanic replacement reaction between Ag tetrahedra and $HAuCl_4$ solution. The surface plasmon resonance (SPR) of gold tetrananocages was tuned from 412 nm to 850 nm through controlling the volume of $HAuCl_4$ solution added. This Au tetrananocage can effectively convert NIR light into heat when the SPR couples with the exciting light. When cancer cells are cultured with the gold tetrananocages for several hours and irradiated, the gold tetrananocages destroy the cancer cells effectively and demonstrate themselves to be a good candidate for combating cancer.

Keywords: tetrananocage, photothermal effect, nanoparticles, near-infrared radiation

PACS: 75.75.–c, 78.20.nb **DOI:** 10.1088/1674-1056/22/9/097502

1. Introduction

Gold nanocages have a great potential in the field of cancer therapy because of the photophysical property of converting light into heat. Combating cancer with nanoparticle-based therapies has gained much attention in recent years.[1–3] Nanoparticles work as light absorbers and produce localized high temperatures to kill tumor cells. The plasmonic resonance wavelength of the nanoparticles must be located in the near-infrared (NIR) region (605–950 nm), because the NIR laser is absorbed less by biological tissues and the typical penetration depth of the NIR light can be several centimeters in biological tissues.[4,5]

Surface plasmons are charge density oscillations confined to metal nanoparticles and metallic nanostructures. When metal nanoparticles are irradiated with electromagnetic radiation of the appropriate wavelength, the surface plasmon resonance (SPR) of the conduction band electrons takes place and leads to strong light absorption and scattering; and simultaneously the local electromagnetic fields near the metal particles are significantly enhanced. The SPR has been studied for a wide variety of potential applications, such as enhanced photothermal therapy,[4–8] enhanced fluorescence,[9–14] and enhanced light-emitting diodes.[15,16] Metal nanocrystals are the major class of nanoparticles with tunable optical absorption behaviors. It is known that several metallic nanoparticles, such as Au, Ag, Cu, and Pt, exhibit plasmonic resonance in the visible and NIR regions of the spectrum, and the plasmonic resonance of these metallic nanostructures is strongly dependent on the composition of the metal, the dielectric function of the surrounding medium, and the size of the particle. The metallic nanoparticles can convert light energy into heat via non-radiative electron relaxation dynamics, endowing them with intense photothermal properties. Such localized heating effects can be directed toward the eradication of diseased tissue, providing a noninvasive alternative to surgery. In the past decade, since Halas's research group first applied a coating of gold nanoshells on solid silica spheres for tumor ablation,[17] a series of NIR-light-absorbing plasmonic nanomaterials have been fabricated to kill tumorigenic cells without damaging normal cells, such as gold nanorods,[18,19] gold nanocages,[20] Au_xAg_{1-x} dendrites,[21] gold nanoshells on polystyrene spheres,[22] assembled gold nanoparticles,[23] and many multifunctional nanocomposites.[24–26] Gold nanocages using Ag nanocubes as sacrificial templates have been demonstrated to have a good efficiency to destroy cancer cells.[27,28] Xia's research group has found that the preparation of Ag nanocubes by this sulfide-mediated method is highly sensitive to the concentration of Na_2S used. There is an unavoidable uncertainty in the Na_2S concentration because this solid is extremely hydroscopic, with commercial sources containing unknown/inhomogeneous quantities of absorbed water.[29]

In the present work, we develope a new one-step approach to synthesizing gold tetrananocages by using silver tetrahedra as the sacrificial templates. The SPR features of the gold tetrananocages are controlled in the spectral region from 400 nm to 850 nm. The method is easy to perform and

*Project supported by the National Natural Science Foundation of China (Grant Nos. 51272246 and 81172082) and the Fundamental Research Funds for the Central Universities of China (Grant No. 2030000001).

†Corresponding author. E-mail: lx-zhu@163.com
‡Corresponding author. E-mail: xlxu@ustc.edu.cn

© 2013 Chinese Physical Society and IOP Publishing Ltd

highly repeatable, and its cycle is short. After cancer cells are cultured with a gold tetrananocage solution for 4 h, a 808-nm near-infrared laser system with a given power intensity and irradiation time is harnessed to excite the thermal nano-absorber gold tetrananocages. The temperature of the culture solution can increase by 20 °C which is high enough to destroy the cancer cells.

2. Experiment

2.1. Material

Absolute ethanol (99.7%, AR), deionized water (18.25 $M\Omega{\cdot}cm^{-1}$), polyvinylpyrrolidone (PVP, MW = 130000, Sigma), silver nitrate ($AgNO_3$, 99.9%, AR), N,N-dimethylformamide (DMF, 99.9%, AR), chloroauric acid ($HClAu_4$, 99.9%, Aldrich), sodium chloride (NaCl, AR), Poly (ethylene glycol) methyl ether thiol (mPEG-Thiol, MW = 5000, Sigma), phosphate buffered saline (PBS, AR), living A549 lung carcinoma and SK-BR-3 cancer cells (Anhui Medical University) were used. The other reagents were of analytical grade and used without further purification. All cell culture media and supplements were obtained from Anhui Medical University.

2.2. Synthesis of silver tetrahedra

Silver tetrahedra were synthesized by a liquid-phase reduction of $AgNO_3$ with the assistance of PVP on a large scale. First, 15 ml DMF was refluxed at 140 °C for 30 min. Then 0.024 g $AgNO_3$ and 0.156 g PVP (MW = 1300000) were dissolved in 14 ml DMF. The mixture was injected into the DMF solution drop by drop. After injection, the reaction solution was kept at 140 °C for 3 h. The product was naturally cooled down to room temperature and purified by centrifugation with ethanol repeatedly.

2.3. Gold tetrananocage synthesis

Gold tetrananocages were prepared through galvanic replacement between silver tetrahedron solution and $HAuCl_4$ solution. Then, 1 ml silver tetrahedron solution was dissolved in 10 ml deionized water and refluxed for 20 min at 100 °C. Different volumes of $HClAu_4$ solution (4 mM) was added dropwise to the silver tetrahedron solution by using a peristaltic pump. The suspension was then stirred at 100 °C until the complete dissolution of the $HAuCl_4$ solution. Once it cooled down to room temperature, AgCl precipitates were found to settle at the bottom of the container. Then the precipitates were removed by dissolving them with a saturated solution of NaCl. After that, the solution was washed with deionized water several times to remove excess PVP and NaCl. Then the sample was re-dispersed in deionized water. Subsequently, 30 mg of mPEG-Thiol was dissolved in 30 ml deionized water and stirred for 30 min at room temperature. Quickly, 4 ml of gold tetrananocages was added into the mPEG-Thiol solution and mixed for 24 h in darkness under vigorous magnetic stirring. The sample was centrifuged and dispersed in a PBS buffer for further characterization and usage.

2.4. Cancer cell culture with Au tetrananocages

Living A549 lung carcinoma cells and SK-BR-3 cancer cells were obtained from Anhui Medical University. They were cultured in Dulbecco's modified Eagle's medium (DMEM) with 10% fetal bovine serum (FBS), 1% penicillin, and 1% amphotericin B at 37 °C in 5% CO_2 (v/v). The medium was changed two or three times a week. The day before treatment with gold tetrananocages, cells were seeded in 35 mm culture dishes at a confluency of 70%–80%. On the treatment day, the cells in serum-supplemented media were treated with the gold tetrananocages for 3 h. A fiber-coupled laser integrated unit with wavelength 808 nm was used for the laser irradiation experiment (see the NIR optical setup in Fig. 1). After the cells were irradiated for 15 min using the 808 nm laser with a spot size of 1.2 cm in diameter, cells were stained with Cein-Am and EthD-1 assay to examine their viability under fluorescent microscopy.

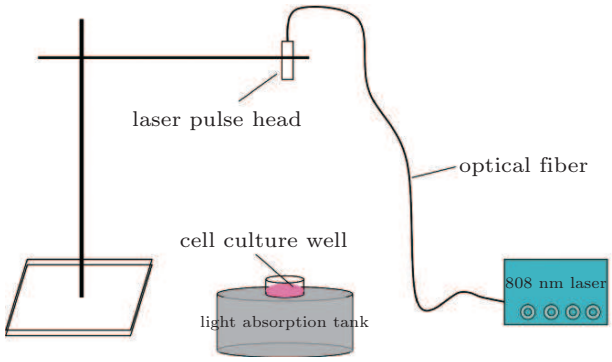


Fig. 1. (color online) Schematic diagram of the NIR optical setup.

2.5. Characterization

The UV–visible absorption spectra were measured using a Shimadzu UV-2401 spectrophotometer. Microstructure and dimensions of the nanoparticles were determined by a JEM-1400 transmission electron microscope (TEM) with an acceleration voltage of 120 kV. Cells were imaged using Olympus fluorescence microscope.

3. Results and discussion

The DMF reduction was applied to synthesize high-quality Ag tetrahedra in the presence of PVP. Detailed procedures are given in the experimental section. Figure 2(a) shows the typical TEM images of silver tetrahedra. Besides the silver tetrahedra, two silver tetrahedra have grown into a silver hexahedron. The black line of Fig. 3(a) shows a typical UV–visible absorption spectrum of the Ag tetrahedral nanoparti-

cles. Three bands located at 353 nm (weak), 399 nm (weak), and 517 nm (strong) are observed. The peaks at 353 nm and 399 nm are attributed to the out-of-plane quadrupole and dipole resonances of the Ag tetrahedral nanoparticles, respectively. While the peak at 517 nm is assigned to the in-plane dipole resonances of the Ag nanoparticles.[30]

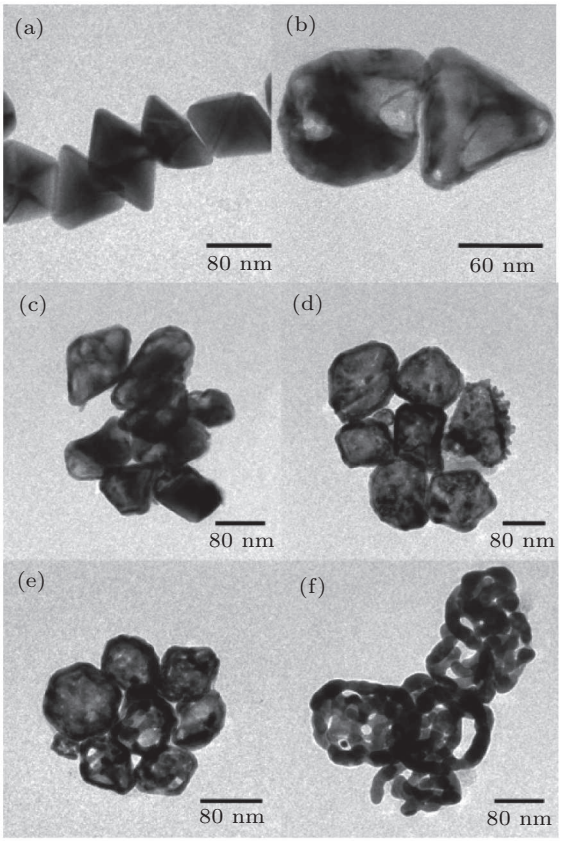


Fig. 2. (color online) TEM images of silver tetrahedra solution (a) before and ((b)–(f)) after the silver tetrahedra are reacted with different volumes of 1 mM $HAuCl_4$ solution: (b) 0.4 mL, (c) 0.6 mL, (d) 1.2 mL, (e) 2.0 mL, (f) 2.5 mL.

Gold tetrananocages are obtained by a replacement reaction, reducing the $HAuCl_4$ precursor with silver tetrahedra $3Ag(s) + AuCl_4^-(aq) \rightarrow 3Ag^+(aq) + Au(s) + 4Cl^-(aq)$. Since the standard reduction potential of an $AuCl_4^-/Au$ pair (0.99 V vs. standard hydrogen electrode, SHE) is higher than that of the Ag^+/Ag pair (0.80 V vs. SHE), silver is oxidized into Ag^+ when silver nanostructures and $HAuCl_4$ are mixed in an aqueous medium.[31,32] All the major steps involved in the galvanic replacement process are outlined in Fig. 4. The TEM images (Fig. 2) are used to follow the morphological and structural changes involved in various stages of the replacement reaction between silver tetrahedra and $HAuCl_4$. There are two steps in the replacement reaction. In the first step, seamless hollow structures are formed with the walls made of Au–Ag alloy (Figs. 2(b)–2(d)). Seen from Fig. 2(b), when a small amount of $HAuCl_4$ solution is dropped into the silver tetrahedron solution, holes are formed at the site of the lowest surface energy. When the volume of the $HAuCl_4$ solution is increased (Fig. 2(c)), the tetrahedra become Au–Ag alloyed shells with hollow interiors. As the amount of $HAuCl_4$ solution increases (Fig. 2(d)), the alloyed shells become thick and the holes shrink due to a combination of volume diffusion, surface diffusion, and/or dissolution and deposition, promoted at 100 °C.[33] In the second step, hollow structures and porous walls are formed via dealloying (Figs. 2(e)–2(f)). When 2.0 ml $HAuCl_4$ solution is added into the silver tetrahedron solution (Fig. 2(e)), pores appear in the Ag–Au alloyed shell again. With more $HAuCl_4$ solution added, the Ag–Au alloyed shell collapses into small fragments (Fig. 2(f)). In order to get more information about the galvanic replacement reaction between silver tetrahedron and aqueous $HAuCl_4$ solution, the absorption spectra are measured and shown in Figs. 3(a) (first step) and 3(b) (second step). In the first step, the absorption wavelength increases from 512 nm to 771 nm due to the deposition of thin gold layers on the surfaces of silver templates and the increase of the Ag–Au alloyed shell thickness. In the second step, when 2.0 ml $HAuCl_4$ is added to the silver solution, the peak shifts to exceed 850 nm due to the increase of the pore's size. When 2.5 ml $HAuCl_4$ solution is used to react with the silver solution, the absorption peak is blue-shifted to 512 nm instead, because the Ag–Au alloyed shell collapses into gold fragments (Fig. 2(f)). Due to the minimal autofluorescence and absorbance from biological specimens in the NIR regions (the transparent window of soft tissues),[34]

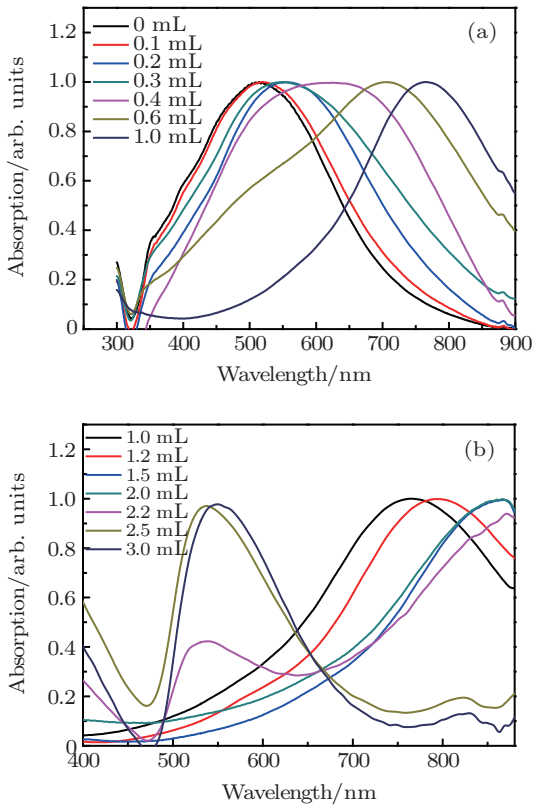


Fig. 3. (color online) UV–visible–near-IR absorption spectra of silver tetrahedra solution before and after reacting with different volumes of 1 mM $HAuCl_4$ aqueous solution.

gold tetrananocages with SPR ranging from 512 nm to 850 nm can be used in photothermal cancer therapy. In our experiment, Au tetrananocages with SPR of 808 nm are taken as a model to investigate the photothermal effect due to their coupling with the emission wavelength of laser. Energy-dispersive X-ray (EDX) data (Fig. 5) confirm that the Au tetrananocage with SPR of 808 nm is consisted of elements Ag and Au with an atomic ratio of 2.37:1.

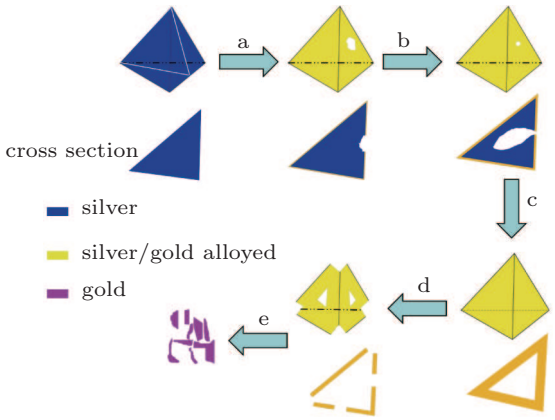


Fig. 4. (color online) Schematic diagram of morphological and structural evolution during the galvanic replacement reaction between silver tetrahedra and $HAuCl_4$ solution.

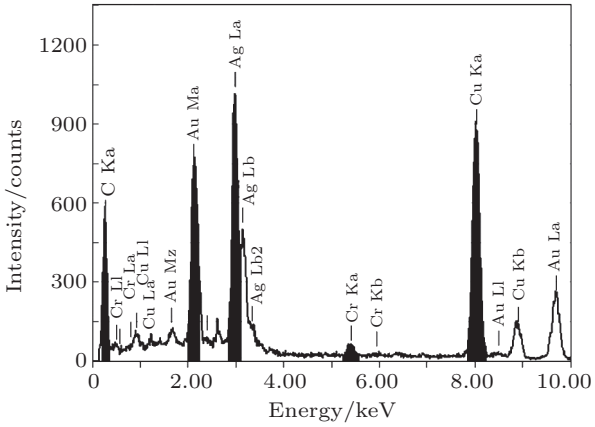


Fig. 5. Energy-dispersive X-ray spectrum for Au tetrananocages with SPR of 808 nm.

The NIR photothermal conversion is sensitive to the concentration of the gold tetrananocages in both *in vitro* and *in vivo* applications. In this section, we investigate the temperature elevation of aqueous gold tetrananocage with different concentration (0–500 pmol/L) under the irradiation of 808 nm laser with a power density of 2 W·cm^{-2}, as shown in Fig. 6. The temperature of the solution in the absence of the gold tetrananocages is increased by only 1.6 °C after the irradiation for 15 min. Such a little temperature increase should not cause any adverse effects to the cells or tissues because the suspension temperature is still below 42 °C a threshold temperature that will cause biomacromolecules (e.g., proteins) to denature.[35] In comparison, the temperature of the sample containing the 500 pmol/L gold tetrananocage aqueous solution is raised from 28 °C to 47.3 °C after irradiation. Such a photothermal effect induced by the NIR SPR absorption is enough to generate thermal damage to the targeted tissue.

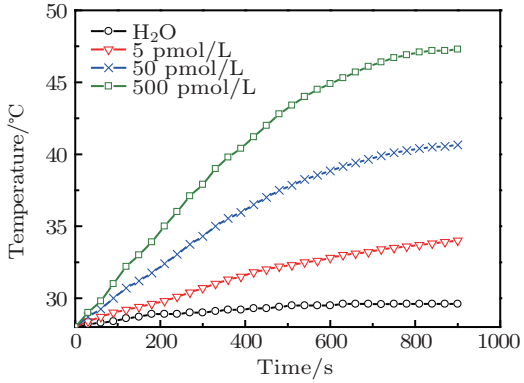


Fig. 6. (color online) Temperature elevation of the aqueous dispersion of gold tetrananocages with different concentration as a function of irradiation time. Water is used as a control.

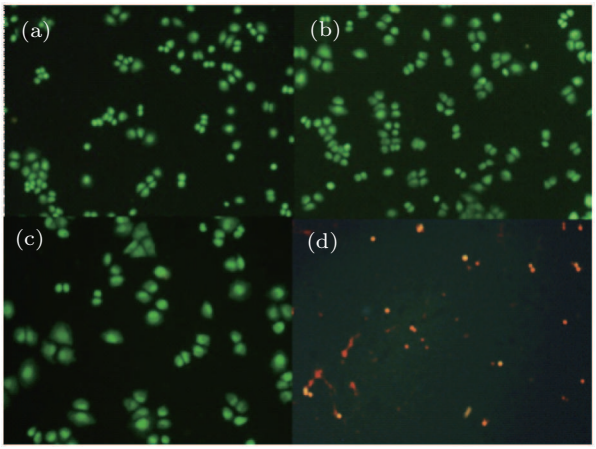


Fig. 7. (color online) Qualitative analysis of the photothermal effect of gold tetrananocages on living A549 lung carcinoma cells. Panels (a)–(d) are the images of the carcinoma cells treated with different parameters: (a) without Au tetrananocages and with irradiation, (b) with neither Au tetrananocages nor irradiation, (c) with Au tetrananocages and without irradiation, (d) with both Au tetrananocages and irradiation.

In the present work, cancer cells (living A549 lung carcinoma cells and SK-BR-3 cancer cells) are used as model tissues to investigate *in vitro* photothermal ablation capability of gold tetrananocages (Figs. 7 and 8, the green fluorescence is Cein-Am used to stain live cells and the red fluorescence is EthD-1 used to label dead cells). No apparent cell death is observed upon treatment without gold tetrananocages (Fig. 7(a)) under the irradiation of 808 nm laser with the power density of 2 W·cm^{-2} over a period of 15 min, which is similar to the sample with neither gold tetrananocages nor irradiation (Fig. 7(b)); while most of the cells are dead as determined by staining with EthD-1 in the presence of the gold tetrananocages with a concentration of 500 pmol/L (Fig. 7(d)). Figure 7(a) verifies that the heat energy from the laser is not

high enough to kill the lung cancer cells in 15 min. Almost all of the cancer cells remain alive in Fig. 7(c), which shows the result with gold tetrananocages without irradiation, indicating that the gold tetrananocages have low biotoxicity to the cancer cells. The gold tetrananocages are not only used for destroying living A549 lung carcinoma cells, a number of different types of cancer cells can be killed as well, such as the breast cancer. The SK-BR-3 cancer cells remain alive after being injected with PBS buffer instead of gold tetrananocage solution (Fig. 8(a)), while lots of breast cancer cells are dead with gold tetrananocages under irradiation (Fig. 8(b)). Therefore, the gold nanocages have a great potential to be used as an ideal photothermal coupling agent in cancer therapy.

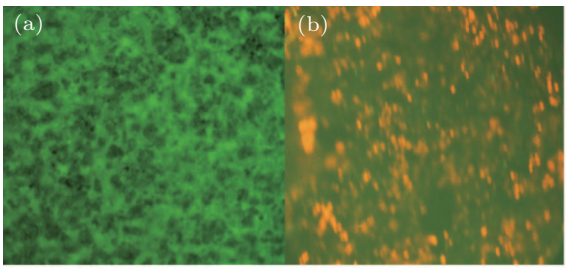


Fig. 8. (color online) Images of the SK-BR-3 cancer cells (a) before and (b) after treatment with irradiation of 808 nm laser with power density of 2 W·cm^{-2} over a period of 15 min.

4. Conclusion

In summary, we have successfully synthesized gold tetrananocages based on silver tetrahedra as sacrificial templates and demonstrated that the nanocage is an efficient laser-driven photothermal agent for the ablation of cancer cells. The absorption peak can be easily tuned to the near-infrared region, the light range in which the tissue has a high degree of penetration. When the cancer cells are injected with the gold tetrananocages and irradiated for 15 min, lots of cancer cells die due to the hyperthermia of the gold nanocages. These results demonstrate the potential of using gold tetrananocages for applications in cancer therapy.

References

[1] Chen J Y, Wiley B, Li Z Y, Campbell D, Saeki F, Cang H, Au L, Lee J, Li X D and Xia Y N 2005 *Adv. Mater.* **17** 2255
[2] Tian Q W, Tang M H, Sun Y G, Zou R j, Chen Z G, Zhu M F, Yang S P, Wang J L, Wang J H and Hu J Q 2011 *Adv. Mater.* **23** 3542
[3] Fan Z, Shelton M, Singh A K, Senapati D, Khan S A and Ray P C 2012 *ACS Nano* **6** 1065
[4] Chen W R, Adams R L, Carubelli R and Nordquist R E 1997 *Cancer Lett.* **115** 25
[5] Chen W R, Adams R L, Higgins A K, Bartels K E and Nordquist R E 1996 *Cancer Lett.* **98** 169
[6] Bardhan R, Chen W X, Perez-Torres C, Bartels M, Huschka R M, Zhao L L, Morosan E, Pautler R G, Joshi A and Halas N J 2009 *Adv. Funct. Mater.* **19** 3901
[7] Cho E C, Zhang Q and Xia Y N 2011 *Nature Nanotechnology* **6** 385
[8] Lukianova-Hleb E Y, Hanna E Y, Hafner J H and Lapotko D O 2010 *Nanotechnology* **21** 085102
[9] Cheng P H, Li D S, Yuan Z Z, Chen P L and Yang D R 2008 *Appl. Phys. Lett.* **92** 041119
[10] Chen Y, Munechika K, Plante I J, Munro A M, Skrabalak S E, Xia O and Ginger D S 2008 *Appl. Phys. Lett.* **93** 053106
[11] Yin N Q, Liu L, Lei J M, Liu Y S, Gong M G, Wu Y Z, Zhu L X and Xu X L 2012 *Chin. Phys. B* **21** 116101
[12] Pompa P P, Martiradonna L, Torre A D, Sala F D, Manna L, Vittorio M D, Calabi F, Cingolani R and Rinaldi R 2006 *Nat. Nanotechnol.* **1** 126
[13] Zhao C H, Zhang B P and Shang P P 2009 *Chin. Phys. B* **18** 5539
[14] Liu L, Xu X L, Lei J M and Yin N Q 2012 *Chin. Phys. Lett.* **29** 017801
[15] Kwon M K, Kim J Y, Kim B H, Park I K, Cho C Y, Byeon C C and Park S J 2008 *Adv. Mater.* **20** 1253
[16] Cho C Y, Kwon M K, Lee S J, Han S H, Kang J W, Kang S E, Lee D Y and Park S J 2010 *Nanotechnology* **21** 205201
[17] Hirsch L R, Stafford R J, Bankson J A, Sershen S R, Rivera B, Price R E, Hazle J D, Halas N J and West J L 2003 *Proc. Natl. Acad. Sci. USA* **100** 13549
[18] Huang X H, El-Sayed I H, Wei Q and El-Sayed M A 2006 *J. Am. Chem. Soc.* **128** 2115
[19] Kuo W S, Chang C N, Chang Y T, Yang M H, Chien Y H, Chen S J and Yeh C S 2010 *Angew. Chem. Int. Ed.* **122** 2771
[20] Chen J Y, Glaus C, Laforest R, Zhang Q, Yang M X, Gidding M, Welch M J and Xia Y N 2010 *Small* **6** 811
[21] Hu K W, Huang C C, Hwu J R, Su W C, Shieh D B and Yeh C S 2008 *Chem. Eur. J.* **14** 2956
[22] Liu H Y, Chen D, Tang F Q, Du G J, Li L L, Meng X W, Liang W, Zhang Y E, Teng X and Li Y 2008 *Nanotechnology* **19** 455101
[23] Wang S T, Chen K J, Wu T H, Wang H, Lin W Y, Ohashi M, Chiou P Y and Tseng H R 2010 *Angew. Chem. Int. Ed.* **49** 3777
[24] Kim J, Park S, Lee J E, Jin S M, Lee J H, Lee I S, Yang I, Kim J S, Kim S K, Cho M H and Hyeon T 2006 *Angew. Chem. Int. Ed.* **45** 7754
[25] Kim J, Lee J E, Lee J, Jang Y, Kim S W, An K, Yu J H and Hyeon T 2006 *Angew. Chem. Int. Ed.* **45** 4789
[26] Wang C G, Chen J J, Talavage T and Irudayaraj J 2009 *Angew. Chem. Int. Ed.* **48** 2759
[27] Skrabalak S E, Chen J Y, Sun Y G, Lu X M, Au L, Cobley C M and Xia Y N 2008 *Acc. Chem. Res.* **41** 1587
[28] Hu M, Chen J Y, Li Z Y, Au L, Hartland G V, Li X D, Marquez M and Xia Y N 2006 *Chem. Soc. Rev.* **35** 1084
[29] Skrabalak S E, Au L, Li X D and Xia Y N 2007 *Nature Protocols* **2** 2182
[30] Gao Y, Jiang P, Song L, Wang J X, Liu L F, Liua D F, Xiang Y J, Zhang Z X, Zhao X W, Dou X Y, Luo S D, Zhou W Y and Xie S S 2006 *Journal of Crystal Growth* **289** 376
[31] Sun Y G and Xia Y N 2004 *J. Am. Chem. Soc.* **126** 3892
[32] Lin W, Warren T H, Nuzzo R G and Girolami G S 1993 *J. Am. Chem. Soc.* **115** 11644
[33] Sieradzki K J 1993 *Electrochem. Soc.* **140** 2868
[34] Tsay J M, Pflughoefft M, Bentolila L A and Weiss S 2004 *J. Am. Chem. Soc.* **126** 1926
[35] Roti J L 2008 *Int. J. Hyperthermia* **24** 3